WP15ER-CPR(17) 18031

A De Backer et al.

Hydrogen interaction with interstitial defects and dislocation loops from atomistic to mesoscopic scales in BCC tungsten

Preprint of Paper to be submitted for publication in Proceeding of 16th International Conference on Plasma-Facing Materials and Components for Fusion Applications

This work has been carried out within the framework of the EUROfusion Consortium and has received funding from the Euratom research and training programme 2014-2018 under grant agreement No 633053. The views and opinions expressed herein do not necessarily reflect those of the European Commission.

Hydrogen interaction with interstitial defects and dislocation loops: from atomistic to mesoscopic scales in BCC tungsten

A. De Backer[1], D.R. Mason[1], C. Domain[2], D. Nguyen-Manh[1], M.C. Marinica[3], L. Ventelon[3], C.S. Becquart[4], and S.L. Dudarev[1]

[1] *CCFE, Culham Science Centre, UK Atomic Energy Authority, Abingdon, OX14 3DB, United Kingdom*

[2] *EDF Lab Les Renardieres, Dpt MMC, F-77250 Moret sur Loing, France*

[3] *DEN-Service de Recherches de Métallurgie Physique, CEA, Université Paris-Saclay, F-91191 Gif-sur-Yvette, France*

[4] *UMET, UMR 8207, Université Lille I, ENSCL, F-59655 Villeneuve d'Ascq, France*

Abstract

In a fusion tokamak, the plasma interacts with the metallic wall and the divertor. Hydrogen atoms penetrate, diffuse, interact with defects in the material, where they are trapped and released. Neutrons produced by the fusion reactions in the plasma are stopped in the material, creating defects, for example vacancy and interstitial clusters, and dislocation loops. Trapping of H in vacancies has been extensively investigated. In this work, we study H trapping and accumulation in interstitial defects, dislocation loops and dislocation lines. These defects have long-range elastic field that attracts H atoms, in agreement with Linear Elasticity theory. In a perfect lattice, H occupies a tetrahedral site of the body centred cubic crystal and interacts with four W atoms. In the core of an interstitial defect, the atomic environment is altered because of strong local deformation. Trapped H atoms in the core of such defects interact with five W atoms, and Density Functional Theory (DFT) is necessary to correctly capture the electronic aspect of H-defect interactions. We have investigated the increase of the binding energy with defect size. Also, the larger the defect, the larger is the number of trapping sites, resulting in H atoms forming a Cottrell atmosphere. We propose a simple two-shell model of H interaction with a defect, including its core and elastic field around the defect. We show that a pairwise approach is valid where a pair consists of one H atom and a defect as a whole, and where close H-H pairs are excluded. The model is valid for loops of any size, can be extrapolated to line edge dislocations and can predict the number of H atoms trapped by defects at finite temperature at equilibrium with H dissolved in the bulk. In plasma relevant conditions, H trapping on a dislocation loop and a dislocation line is significant but depends on H concentration in the bulk, and also on the kinetic processes that are not described in this work.

1. Introduction

Hydrogen retention in a metal depends on its microstructure and porosity, and the presence of defects such as grain boundaries, dislocations or precipitates. Microstructure evolves under ion and neutron irradiation. Figure 1 of Ref. [1] shows a large density of dislocation loops formed in tungsten under ion irradiation. Exposure of pristine tungsten to high flux plasma also creates dislocations and nano-cavities, observed in the vicinity of dislocations [2]. H concentration close to the surface is higher than the H solubility limit in W [3] and this suggests that high H concentration triggers defect formation. Many papers describe hydrogen interaction with vacancies in tungsten [4-6], which are strong traps. But relatively little is known about H interaction with self-interstitial atoms (SIA), loops and dislocations. Early work gave the maximum binding energy of a H atom to a single SIA, which is an extra atom in a crystal lattice [4]. Interstitial type dislocation loops form by clustering of SIAs as platelets, characterised by various Burgers vectors. One

consequence of this process is the formation of long range elastic fields. A H atom produces small dilatation in the lattice and interactions with elastic fields of interstitial defects. Experimental results showing synergy between H retention and damage production during co-irradiation has been reported recently [7]. During co-irradiation, H atoms, vacancy and interstitial defects interact and the interpretation of resulting H retention requires characterisation of trapping of H atoms in the elastic fields of extended interstitial type traps. In what follows, we describe our two shell (TS) model (involving interaction in the elastic “shell” and core “shell”) and, briefly, H interaction in the elastic shell detailed in [8]. Secondly, we describe H interaction in the core shell using DFT, giving an expression for H binding energy as a function of defect size. In the third section we justify the pairwise approach of our TS model for H accumulation in defects, using also the DFT results. Finally we discuss how to take into account the temperature effects.

2. The two shell model

The smallest SIA defect is formed by 2 atoms sharing one atomic site. In BCC tungsten, they form a dumbbell (also sometimes called a crowdion) aligned along a [111] direction. Clustering of SIAs is highly energetically favourable and they form platelets, or dislocation loops, with the Burgers vector parallel to [111]. Linear Elasticity (LE) theory gives an analytical expression of H interaction with the long range elastic field created by a loop [9], in cylindrical polar coordinates

$$E_b(\mathbf{r}) = -P(\mathbf{r})\Omega^H_{rel} = -A\frac{\mu b}{3\pi}\frac{1+\nu}{1-\nu}\frac{3\cos^2(\theta)-1}{2r^3}\Omega^H_{rel} \quad (1)$$

where μ = 0.99 eV/Å^3 and ν = 0.28 are the shear modulus and the Poisson ratio of W, b and A are the Burgers vector and the area of the loop, Ω_{rel}^H is the relaxation volume of a H atom. The strength of interaction decreases as a function of distance, away from the loop, and is attractive or repulsive depending on angle θ. At short distances, a more complex expression is necessary (detailed in [10]) because of the finite dimensions of the loop. Comparison between both expressions is given in [8] and Figure 1 only shows the iso-contours of binding energy of H in the vicinity of a loop, in a plane containing the Burgers vector. H produces a dilatation of the lattice and hence is repelled from the inside of the loop. Binding energy is maximum close the core of the loop which is sketched by two hatched regions. Values of binding energy given by Linear Elasticity diverge close to the core where an atomistic approach is required, Density Functional Theory (DFT). In the perfect lattice, DFT predicts that H occupies a tetrahedral site [4] at equal distances from 4 W atoms. This configuration is illustrated in figure 2. Using DFT, we also calculated the H relaxation volume, $\Omega_{rel}^H = 0.15 \times ½\ a_0^3$ (a_0 is the lattice parameter), which is a parameter entering the expression for the binding energy in the elastic shell. This value is smaller than $\Omega_{rel}^{He} = 0.33 \times ½\ a_0^3$, the relaxation volume of a He atom [11].

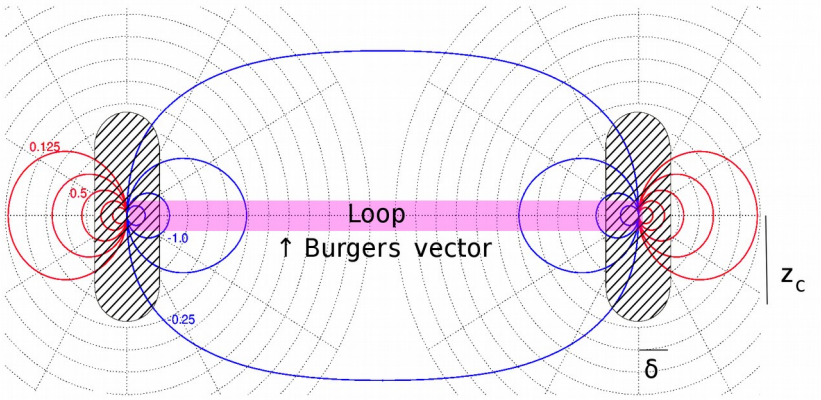

Fig. 1. Iso-contours of the binding energy of a H atom with the elastic field of a dislocation loop in a plane parallel to the Burgers vector (here perpendicular to the plane of the loop). Figure illustrates the two shell (TS) model consisting of elastic shell and the core shell. Red (resp. blue) lines show positive (resp. negative) H binding energy to the loop, computed using Linear Elasticity theory for the elastic shell. The hatched areas shows the core of the defect, which is the second shell of our model and where the lattice is strongly distorted, requiring an atomistic treatment.

3. The core shell

The smallest interstitial defect is a single SIA and in [4] we reported the maximum value of H binding energy for the configuration illustrated in Figure 2b. A dumbbell of W atoms (in dark blue) shares one lattice site. It changes the atomic volume (the colour of W atoms reflects the Voronoi volume computed for W atoms only, in lattice units). The volume is smaller in the [111] direction (blue). H is close to the defect but one of the atoms of the dumbbell is at similar distance to W atoms forming the tetrahedral sites. In total, H has five nearest neighbour (NN) W atoms instead of four as in the perfect lattice. The slight enlargement of the tetrahedral site, due to the relaxation of the lattice because of a SIA, explains the attraction of a H atom to a defect but the “chemical” effect associated with the presence of the 5th W atoms must be taken into account.

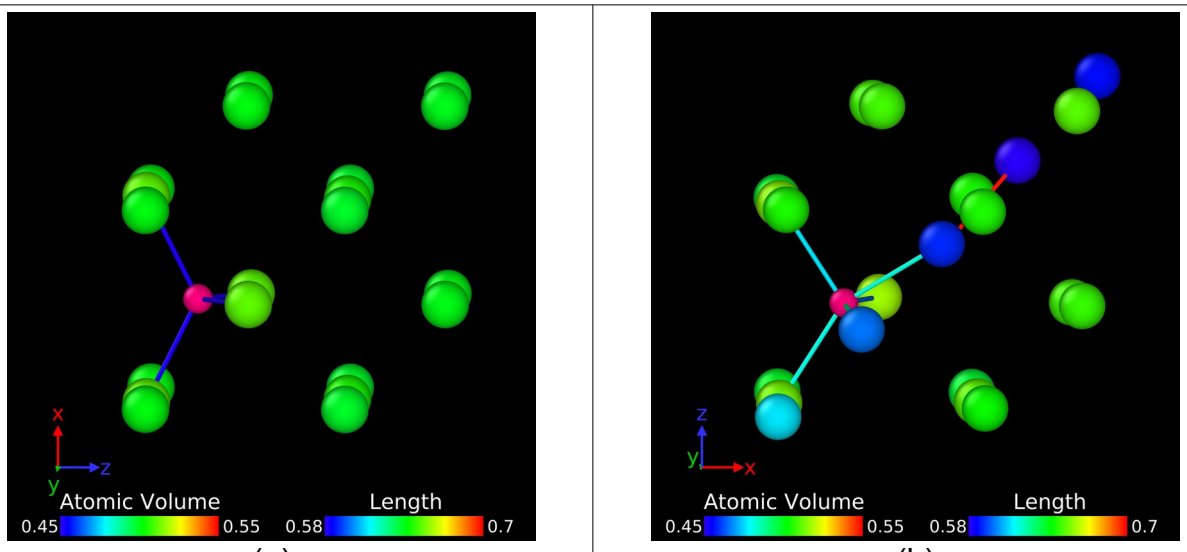

Fig. 2. (a) In perfect bcc lattice, H occupies a tetrahedral site and has 4 nearest neighbours (NN). (b) The presence of a self-interstitial atom (SIA) creates a structure

involving a pair of atoms (linked by a bond shown in red) parallel to [111] and is known as a "dumbbell". The most favourable position of H is at a tetrahedral site the volume of which has been slightly enlarged by the SIA and where one atom of the dumbbell becomes the 5th NN of the hydrogen atom.

The introduction of H in one tetrahedral site of W lattice, with or without defect, can be decomposed into two steps. Firstly, the formation of one enlarged site (ES), pushing the W atoms. Secondly, the introduction of an atomic H, including electronic interaction. The binding energy of H with one mSIA can be decomposed in a similar way, the difference of formation energy of the ES close to mSIA and in perfect lattice and the difference of energy due to electronic interactions. For example, for the 1H.1SIA configuration given figure 2b, the formation of an ES requires 0.14 eV compared to 0.25 eV in a perfect lattice (figure 2a), which is a gain of 0.11 eV. Electronic interactions add 0.16 eV. The binding energy of H with a SIA is 0.27 eV. The smaller formation energy of an ES near the SIA is due to the pre-existing deformation. To analyse the energy gain associated with electronic interactions, we decompose the electronic charge density of *nH.mSIA* as

$$\Delta\rho(nH.mSIA) = \rho(nH.mSIA) - \rho(mSIA^*) - \rho(nH) \quad (2)$$

where $\rho(nH.mSIA)$, $\rho(mSIA^*)$ and $\rho(nH)$ are the electronic charge densities of the *nH.mSIA* defect, the *mSIA* with *m* ES and the n H atoms with the configuration of the *nH.mSIA* [12]. With this definition, the change in electronic density $\Delta\rho(nH.mSIA)$ describes electronic charge transfers (from negative to positive regions).

Figure 3 illustrates equation 2 for the case of a 1H.1SIA configuration (in a plane containing a [111] direction and a H atom). Positions of W (resp. H) atoms are shown in green (resp. grey). Charge densities around W atoms along the [111] direction show an increase of charge density between W atoms due to the deformation of the lattice [13]. The ES is revealed only by the slight asymmetry of the low charge density contour around it. The charge density of a H atom is given by its 1s orbital. In the last picture, electronic charge density deformation consists of a concentration of charge around H from the depleted regions in the ES and small lobe-shaped changes around the nearest W atoms. These indicate a hybridisation of the s-state of H and d-states of W. It is positive toward H which suggests some H-W bounding [14]. In the case of a H in perfect lattice, it has four W atoms at slightly shorter distance and electronic density deformation is larger. Consequently, binding in 1H.1SIA correlates with variation of electronic density. Figure 6b confirms this effect by a plot of electronic density along the H-W lines for the 1H and the 1H.1SIA.

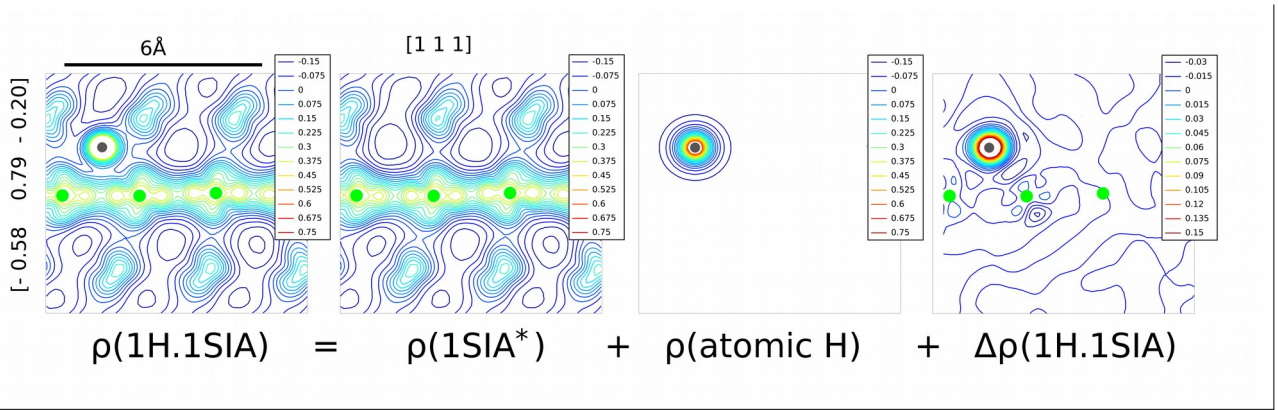

Fig. 3. Illustration of equation 2 for the electronic charge density variation Δρ(1H.1SIA) as a function of the electronic charge densities of the 1H.1SIA, the 1SIA (1SIA with one enlarged site, ES to be occupied by H) and a H atom. Positions of H (resp. W) atoms are shown in grey (resp. green). The electronic charge density deformation map shows a*

concentration of charge around the H atom (due to its s state) and lobe shaped changes around W atoms (due to their d states).

Various defect configurations have been calculated by DFT with VASP [15] using PW91 [16], a cut-off energy of 350 eV, 2×2×2 k-points, with box size up to 9×9×9, performed at a constant volume and corrected using the elastic correction scheme described in [17]. The total binding energy is calculated as

$$E_b(nH.mSIA) = nE_f(H) + E_f(mSIA) - E_f(nH.mSIA) - nE_{ref}. \quad (3)$$

We observed good agreement between LE and DFT values at larger distances from the defect. The maximum binding energy corresponds to the case where H interacts with five W atoms in the core of the defect. The energy increases as a function of defect size to 0.65 eV for the 1H.37SIA. In agreement with DFT results, LE also predicts an increase which can be approximated by the formula $E_b(1H.mSIA)$ *[eV] = 0.1069 ln(19.861m)* assuming the core minor radius of $\delta = 0.4\ a_0$ for any defect size (figure 4a).

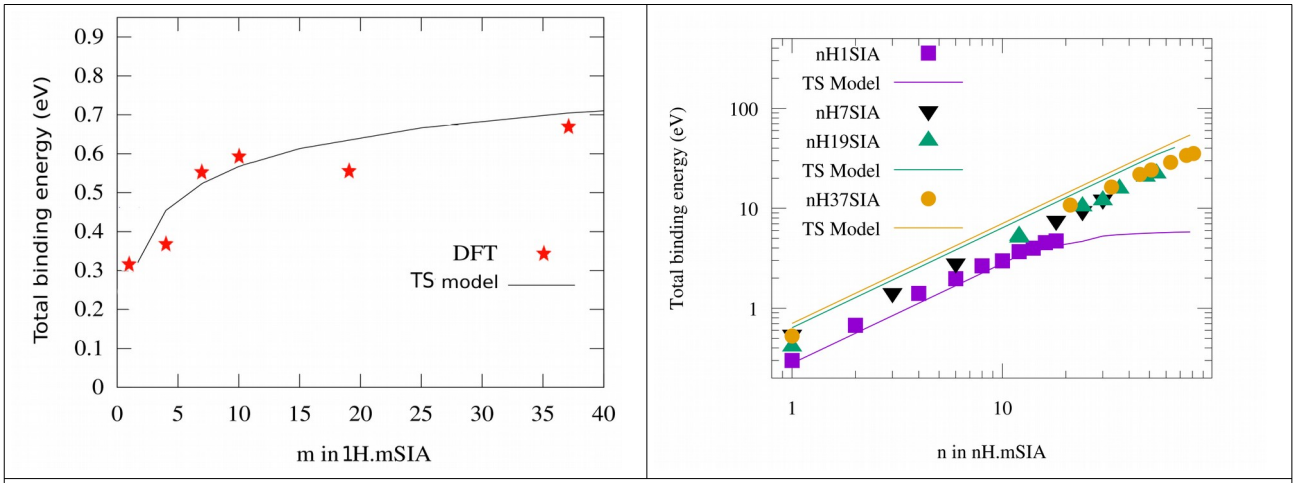

Fig. 4. (a) Binding energy of H in the core of 1SIA, 4SIA cluster and several b=1/2[111] loops predicted by DFT and by our TS model using the core minor radius, $\delta = 0.4\ a_0$. (b) The total binding energy of nH.mSIA calculated by DFT and with the TS Model. Only the maximum values have been retained for these plots.

4. Hydrogen accumulation

For the H accumulation we include a simple pairwise approach in our TS model. The total binding energy is

$$E_b(nH.mSIA) = \sum_{i=1}^{n} E_b((H)_i.mSIA) + \sum_{j>i}\sum E_b((H)_i - (H)_j) + \Delta E_b(nH.mSIA) \quad (4)$$

It is given as a sum of H-defect pair attraction, H-H pair interaction and a "many-body" term by analogy with other pairwise approaches. The first term was defined in the previous sections. In [8], we demonstrated that H-H interaction is mainly a strong repulsion up to ½a_0, where a_0 is the lattice parameter. It is then equivalent to an exclusion principle of any H-H pair in first and second nearest neighbour positions. One contribution to the many body term is the electronic interaction of the 12H.1SIA which is illustrated in figure 6a. Iso-

contours are drawn in a plane containing the [111] direction of the 1SIA axis, and four of the 12 H atoms. Now 6 H atoms interact with each atom of the dumbbell. It enhances the electronic interaction around them and leads to a slight decrease between them. It is also visible in plots of figure 6b where one compares the electronic interaction along the H-W directions. There is no difference on the H side between the 1H.1SIA and the 12H.1SIA but an increase on the W side. However, in our DFT calculations we found that the many body terms in the total binding energy is generally negligible. Many nH.mSIA configurations have been calculated by DFT, decorating mSIA loops with H atoms. First, all the 24 most favourable tetrahedral sites of the SIA taken individually have been selected. Then the sites that are inside the loop have been excluded. H pairs in 1NN and 2NN were also excluded and we favoured alignment of H atoms along [111] direction. Figure 5b shows a 54H.19SIA configuration. In figure 4b, we plotted the maximum total binding energy as a function of the number of H and the defect size by DFT and our TS model. The elongated core parameter z_c = 0.8 a_0 (see figure 1). We see that the total binding energy increases linearly until the core is filled, then starts to saturate because additional H must be at larger distances from the core, reducing the H-defect pair energy (the first term of equation 4). The number of H atoms in the core of a nH.mSIA is proportional to the square root of *m* because it is proportional to the perimeter of the loop, the radius of which is given by $\rho(m) = a_0\sqrt{\frac{m}{\sqrt{3}\pi}}$[8]. Our DFT results follow $n_{1SIA}\sqrt{m}$ and the TS model for large loop gives 7.96√m. Extrapolation to the number of H trapped in the core of an edge dislocation line is $n_d = (0.37/a_0)\, n_{1SIA}$ (per unit length) where 0.37 is a geometric factor. Outside the core, there are more possible trapping sites with lower binding energy. One sees that H atoms form a Cottrell atmosphere of the loop or the dislocation line.

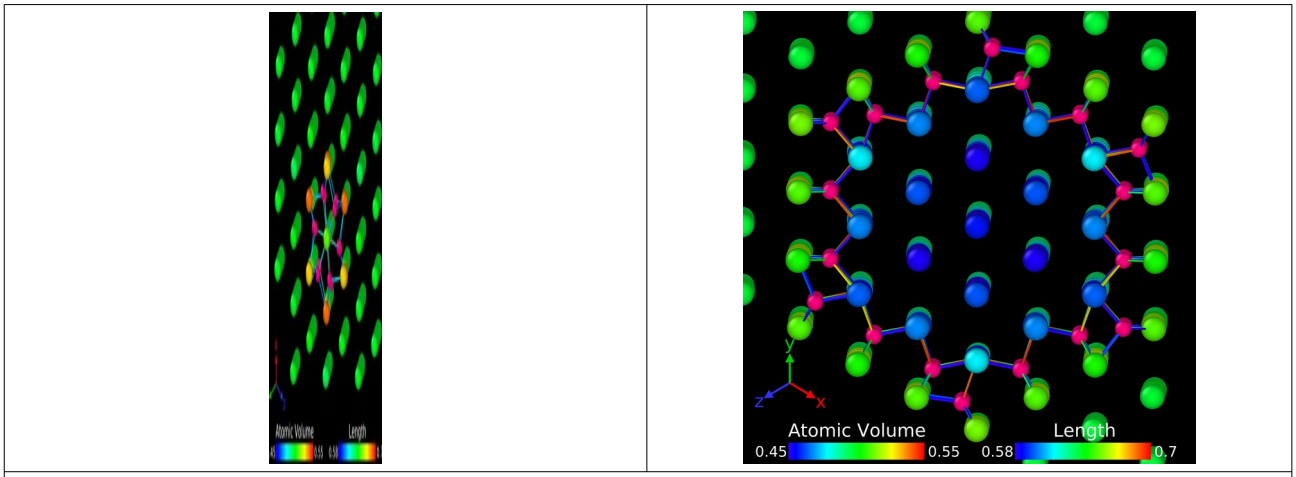

Fig. 5. (a) Illustration of the 12H.1SIA and (b) the 54H.19SIA from the [111] direction. Large atoms are tungsten, coloured according to the Voronoi volume (with W only) and pink atoms are H, with vectors pointing to the 5 nearest neighbour W.

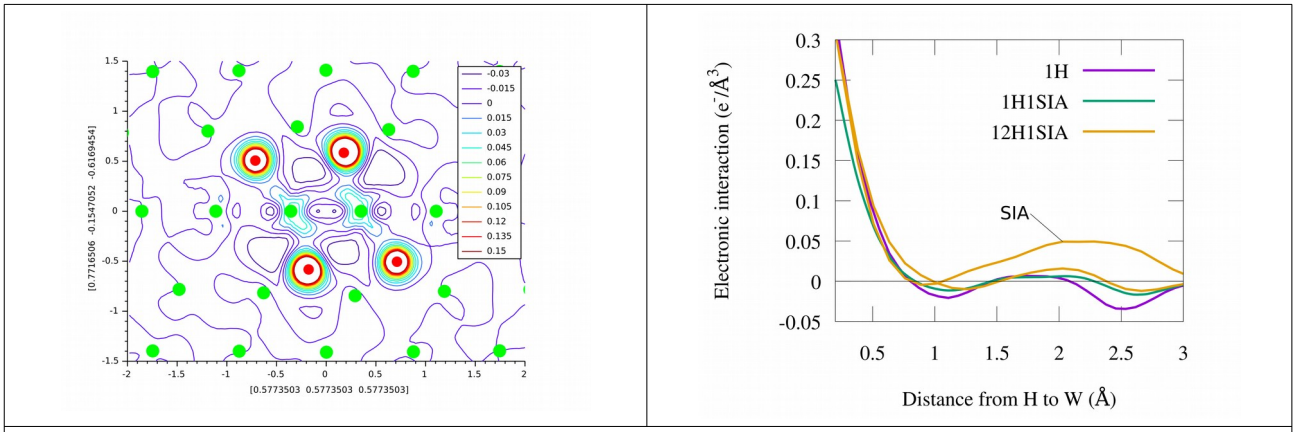

Fig. 6. (a) Electronic interaction (given by equation 2) of the 12H.1SIA (see figure 5a), in a plan containing the [111] direction and 4 of the 12 H atoms. Red (green) atoms are H (W). It shows that the H accumulation enhances the electronic interaction between W and H and reduces it between the W of the dumbbell. (b) Electronic interaction along the H-W direction for H in perfect lattice, the 1H.1SIA and the 12H.1SIA.

5. The temperature effect

At a finite temperature, nH.mSIA defects can adopt many more configurations. In [8], we calculated the free energy of nH.mSIA including the configurational entropy and using our TS model. We also derived simple analytical formulae of the number of H trapped by the defects based on H occupancy probability in all sites given by Fermi statistic and introducing an exclusion volume similarly to the principle of exclusion of the H-H close pair. We characterised the validity conditions of the analytical formulae. Both approaches give the number of H trapped in the core and in the elastic shells of defects of any size, as a function of temperature and at equilibrium with H concentration in the bulk. The later depends on H pressure and, in fusion relevant conditions, on H flux coming from the plasma, then the distance from the surface. With large H flux and close to the surface, H trapping in both shells is significant at room temperature and above. However, under these conditions, our results only describe a “local” equilibrium between the bulk and the defects, where several kinetic processes of diffusion, trapping and release rates interplay.

6. Discussion

H interaction with interstitial defects is controlled by elastic interaction at long distance and the atomic environment in the core. Elastic interactions are fully determined by elastic properties of the material, size and Burgers vector of the defect and H relaxation volume. Inside the core of the defect, H interacts with 5 W atoms instead of 4 in perfect lattice. The larger the defect, the larger is the binding energy. One reason is the smaller formation energy of the enlarged site because of the pre-existing deformation. However, the electronic effects are significant which requires an atomistic approach such as DFT. At 0 K, the accumulation of H first shows a linear increase of the total binding energy due to the occupancy of the core sites. H-H pairs in first and second nearest neighbour positions, meaning at distance smaller or equal to $a_0/2$ must be excluded. Then the sites of the elastic shell are occupied, giving a sub linear increase of the total binding energy. These properties have been illustrated and quantified using a large number of DFT calculations. Additional calculations have investigated the effects of the DFT conditions (e.g. pseudo

potential, exchange correlation functional) because of the sensitivity of the H-defect interaction to electronic charge density, but that do not change the results significantly. We developed and described a pairwise two shell model of H interaction and accumulation with interstitial defect of all size. Real defects do not have a perfect shape and we observed some deviations. For example, large loops do not have their habit plan perpendicular to the Burgers vector. Also, some SIAs at the periphery of the loop are found to be crowdions and not dumbbell. This complicates the treatment of nH.mSIA configurations but we did not observed significant change of the results.
We introduced the effect of temperature on the number of H trapped by one defect at equilibrium conditions with H concentration in bulk. Full calculations are given in details in [8]. However H release in fusion relevant conditions depends on kinetic, i.e. barrier energies, trapping and release rates and mobility of the nH.mSIA.

7. Conclusion

A combination of Linear Elasticity and Density Functional Theory clarified the fundamentals of H interaction with interstitial defects of various sizes. It justified a simple two shell pairwise model with a long range interaction due to the elastic field of the interstitial defect and the strongest interaction within the core of the defect. Main properties of the model are
- decrease of H interaction with distance to the defect core
- increase of the binding energy of 1H.mSIA with the defect size
- H accumulation conditioned by the short H-H pair exclusion
- total binding energy dominated by the H-defect pair interaction.

So far, our model does not include kinetic processes but can predict the number of H trapped in the Cottrell atmosphere of loops and dislocations [8] as a function of temperature at equilibrium with H concentration in bulk.

Acknowledgements
This work was part-funded by the RCUK Energy Programme [grant number EP/P012450/1]. This work has been carried out within the framework of the EUROfusion Consortium and has received funding from the Euratom research and training programme 2014-2018 under grant agreement No 633053. The views and opinions expressed herein do not necessarily reflect those of the European Commission.
This work was supported by EUROfusion Enabling Research project TriCEM (Tritium Retention in Controlled and Evolving Microstructure) and JET3TRI project. MCM acknowledges support from the GENCI -(CINES/CCRT) computer centre under Grant No. A0010906973. Most of atomic structures shown in figures in this poster were illustrated using [18].

References
[1] F. Ferroni, X. Yi, K. Arakawa, S.P. Fitzgerald, P.D. Edmondson, S.G. Roberts, Acta Materialia, 90 (2015) 393.
[2] A. Dubinko, A. Bakaeva, M. Hernández-Mayoral, D. Terentyev, G. De Temmerman, J.-M. Noterdaeme, Physica Scripta, T167 (2016) 014030.
[3] R. Frauenfelder, Journal of Vacuum Science and Technology, 6 (1969) 388.
[4] C.S. Becquart and C. Domain, JNM, 385 (2009) 223.
[5] K. Heinola, T. Ahlgren, K. Nordlund, J. Keinonen, Phys. Rev. B, 82 (2010) 094102.
[6] D. Kato, H. Iwakiri, Y. Watanabe, K. Morishita, T. Muroga, Nuclear Fusion, 55 (2015) 083019.

[7] S. Markelj, T. Schwarz-Selinger, A. Založnik, M. Kelemen, P. Vavpetič, P. Pelicon, E. Hodille, C. Grisolia, Nuclear Materials and Energy, (2016).
[8] A. De Backer, D.R. Mason, C. Domain, D. Nguyen-Manh, M.-C. Marinica, L. Ventelon, C.S. Becquart, S.L. Dudarev, submitted to Nuclear Fusion.
[9] S.L. Dudarev and A.P. Sutton, Acta Materialia, 125 (2017) 425.
[10] D. Mason, X. Yi, M. A. Kirk, S. L. Dudarev, 26 (2014) 375701.
[11] F. Hofmann, D. Nguyen-Manh, M.R. Gilbert, C.E. Beck, J.K. Eliason, A.A. Maznev, W. Liu, D.E.J. Armstrong, K.A. Nelson, S.L. Dudarev, Acta Materialia, 89 (2015) 352.
[12] C. Domain, C. S. Becquart, J. Foct, Phys. Rev. B, 69 (2004) 144112.
[13] P. M. Derlet, D. Nguyen-Mahn, S.L. Dudarev, Phys. Rev. B, 76 (2007) 054107.
[14] D. Nguyen-Manh, A. P. Horsfield, S. L. Dudarev, Phys. Rev. B, 73 (2006) 020101.
[15] G. Kresse and J. Hafner, Phys. Rev. B, 47 (1993) 558.
[16] J.P. Perdew, J.A. Chevary, S.H. Vosko, K.A. Jackson, M.R. Pederson, D.J. Singh, C. Fiolhais, Phys. Rev. B, 46 (1992) 6671.
[17] C. Varvenne, F. Bruneval, M.-C. Marinica, E. Clouet, Phys. Rev. B, 88 (2013) 134102.
[18] A. Stukowski, Model. and Simul. Materials Science and Engineering, 18 (2010) 015012.